Transactions of the Materials Research Society of Japan 29[6] 2767-2772 (2004)

Thermoelectric property of ladder-type oxide $[(Sr_{1-x}Ca_x)_2CuO_3]_\gamma [Cu_{1-y}Co_yO_2]$

Shunsuke Tayama, Yuzuru Miyazaki and Tsuyoshi Kajitani
Department of Applied Physics, Tohoku University, Japan
Fax:81-22-244-7969, e-mail: kajitani@mail.tains.tohoku.ac.jp

Doped two-leg ladder copper oxide, $(Ca_{13.5}Sr_{0.5})Cu_{24}O_{41}$ being an incommesurated layered crystal, exhibits superconductivity in the low temperature, T<12K, and high pressure, P>3GPa, ranges. The end-member oxide, $Sr_{14}Cu_{24}O_{41}$ shows relatively high Seebeck coefficient, S=200 μ V/K at 300K. Present work is aimed to enhance the thermo-electric properties of this two-leg ladder oxide by the partial co-substitution of Co and Ca for the chain site Cu and for the interleaving site Sr, respectively. Optimized chemical content was formulated at x=0.2 and y=0.2 for the title chemical formula while the incommensurate stacking sequence is γ =0.69. Neutron powder diffraction intensities were analyzed by the use of PREMOS for the present 3+1-dimesional spacegroup crystals. The space groups assumed for the end member and the doped ones are Amma(00 γ)ss1 and F222(00 γ)001, respectively. CuO_5 pyramids are partly formed in the Ca-doped crystals, in which the apical oxygen atoms are in the $(Co,Cu)O_2$ chains.

Keywords: ladder-type cuprate, modulated structure, p-type semiconductor, Neutron powder diffraction, Seebeck coefficient

I.INTRODUCTION

A copper oxide $Sr_{14}Cu_{24}O_{41}$ has been known as an end-member of the superconductor $(Ca_{13.5}Sr_{0.5})Cu_{24}O_{41}$ which becomes superconducting state at temperatures lower than 12K under the pressure higher than 3GPa[1]. The Seebeck coefficient of $Sr_{14}Cu_{24}O_{41}$ was reported by Kato et al.[2] as high as 200 μ V/K at 300K. This crystal system has a composite crystal-type[3-8] modulated structure consisting of two different crystal subsystems (layers) , namely, $Sr_2Cu_2O_3$ and CuO_2 layers. The $Sr_2Cu_2O_3$ layer is characterized by the unique pseudo one-dimensional Cu_2O_3 "two-leg ladder-type" square lattice. The CuO_2 layer is the infinite one dimensional chain layer, expected as the insulating layer.

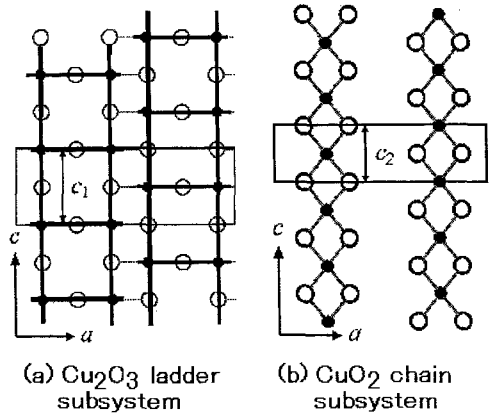

Fig.1 Schematic presentation of Cu_2O_3-ladder and CuO_2-chains.

Figure 1 shows atomic arrangements in above two subsystems. Kato et al.[2] reported that the electrical resistivity of the $Sr_{14}Cu_{24}O_{41}$ increase with decreasing temperature but becomes metallic by the partial substitution of strontium ion with calcium ion. The Seebeck coefficient becomes low in the metallic samples at low temperatures.

High Seebeck coefficient and low electrical resistivity of several cobalt oxides, γ -$NaCoO_2$[9] and $[Ca_2CoO_{3.34}]_{0.614}$ $-[CoO_2]$ (Ca349)[10,11] are noted recently. These oxides are prospective high temperature thermoelectric materials. High Seebeck coefficient of these oxides has been interpreted with the entropy flux of spin and orbital degeneracy in the conduction layers, i.e., CoO_2 triangular layers. Due to the mixed valence states, $Co^{3+}(3d^6)$ and $Co^{4+}(3d^5)$, of the cobalt ions are concluded from the charge neutrality of the two oxides. One charged carrier, i.e., the positive hole in the two cases, could carry S=1/2 spin and orbital ordering of the 3d-electrons by each Co-O-Co hopping.[12,13] In the high temperature regime, the Seebeck coefficient is dominated by the entropy change due to the charge and spin simultaneous flow.

Present study was aimed to improve the thermoelectric property of the two-leg ladder system by the partial substitution of calcium and cobalt ions with strontium and copper ions , respectively. Structural alteration due to the substitution was also a point of interest.

II.EXPERIMENTAL

$[(Sr_{1-x}Ca_x)_2Cu_2O_3]_\gamma$ $[Cu_{1-y}Co_yO_2]$ polycrystalline samples with $x \leqq 0.7$, $y \leqq 0.5$ and $\gamma = 0.69$ were synthesized by the solid state reaction. 3N-CuO, 3N-$SrCO_3$, 4N-$CaCO_3$ and 3N-Co_3O_4 powders were mixed, pelletized and calcined at 960 ℃ for 12 hours in the oxygen gas flow. Calcined pellets were pulverized, palletized and sintered for three times at the same temperature for the homogenization procedure. Powder X-ray and neutron diffraction analyses were performed with the use of RIGAKU-RAD-X (Cu K_a radiation) and JRR3M-HERMES[14], respectively. Rietveld analysis program REMOS[15] was used to analyze the 3+1 dimensional crystal structures. The monochromatized (Ge 331) incident neutron radiation with $\lambda = 1.8196$ Å was used. The collimation of 6'-open-18' was kept during the experiment. The magnetic susceptibility was measured at 1000Oe from 5K to 300K with the use of Quantum Design SQUID magnetometer. The electrical resistivity and Seebeck coefficient were measured from 4K to 300K by the four probe method and the steady heat flow method, respectively. High temperature measurement from 100℃ to 700℃ were performed by the use of an automated resistivity and Seebeck coefficient measurement equipment Ozawa-Kagaku RZ2001i.

III.RESULTS

III-1.SOLUBILITY LIMIT

The single phase region of the calcium and copper substituted polycrystalline samples was determined from the XRD patterns taken at room temperature. Open circles shown in the figure 2 correspond to the single phase region of the $[(Sr_{1-x}Ca_x)_2Cu_2O_3]_\gamma[Cu_{1-y}Co_yO_2]$. The maximum values of the x and y are about 0.8 and 0.5, respectively, at $\gamma = 0.69$. The lattice parameters a and b are common for the two subsystems but the c-axis lengths are different.

Figures 3 and 4 show the lattice parameters vs. calcium content dependency measured by the powder X-ray diffraction measurements at room temperature. The a- and b-axis lengths decrease with increasing calcium content but c_1- and c_2-axis lengths decrease and increase, respectively, with increasing calcium content. These lengths similarly change with increasing cobalt contents, y=0.1, 0.2 and 0.3. There is no appreciable change in a- and b-axis with the change of cobalt content, however. Decrease of a- and b-axis lengths with increasing calcium content may be understood in terms of the difference in the Shannon-Prewitt[16] ionic radii of Sr (r=1.26 Å) and Ca(r=1.12 Å).

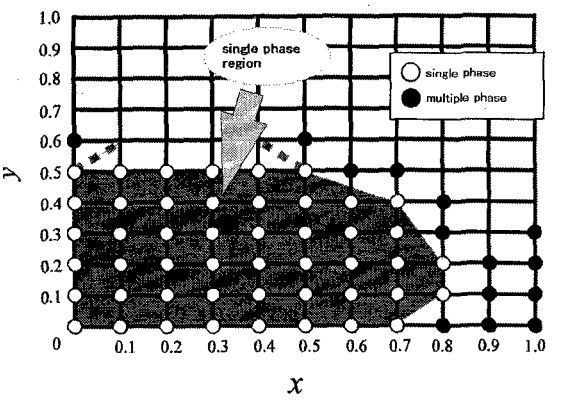

Fig.2 Single phase region of $[(Sr_{1-x}Ca_x)_2Cu_2O_3]_\gamma$ $[Cu_{1-y}Co_yO_2]$ with $\gamma = 0.69$.

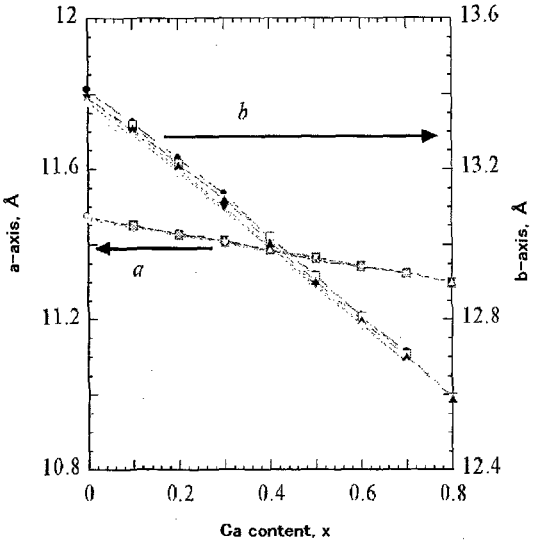

Fig.3 a- and b-axes vs. calcium content dependency at room temperature. ●, □, ◆, ▼ and ○ signs represent cobalt content, y=0.0, 0.1, 0.2, 0.3 and 0.4, respectively.

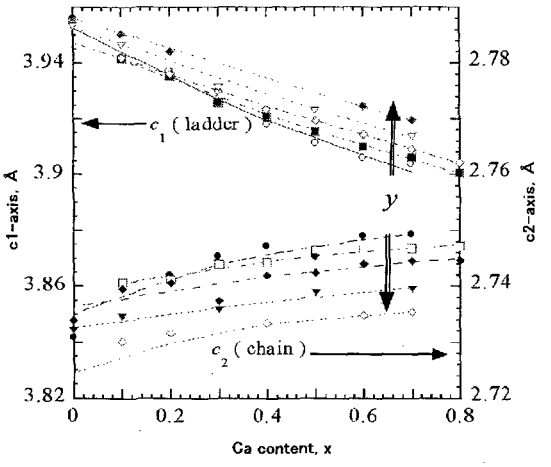

Fig.4 c_1- and c_2-axes vs. calcium content dependency at room temperature. The c_1- and c_2-axes correspond to the unit cell lengths of the "ladder" and "chain" subsystems parallel to the modulation, respectively.

III-2 RIETVELD ANALYSIS

Structure analysis for the XRD and NRD patterns were performed with use of a computer code PREMOS[15]. Two different 3+1 dimensional super spacegroup structure models, i.e. Amma(00γ)ss1 and F222(00γ)001 were assumed. These models were selected by Jensen et al. for the single crystal structure analyses and by Ohta et al.[5] and Isobe et al.[7] for the powder ND analyses. The former and the latter models were assumed for the strontium dominant and calcium rich samples, respectively. In the present powder runs, it was not possible to determine proper model from the systematic presentation of weak superlattice peaks in the powder ND patterns. We compared the residuals, R_{wp}, i.e., weighted residuals for the diffraction patterns, assuming two different models. Table I shows obtained values of the R_{wp} for the samples with x=0 – 0.7 and y=0.0. Obtained structural parameters for $[(Sr_{1-x}Ca_x)_2Cu_2O_3]_\gamma[Cu_{1-y}Co_yO_2]$ with x=0.7 and y=0.0 at 300K are shown in the Appendix.

Table I. R_{wp} of ladder type oxides obtained for the NRD patterns assuming two different structure modes.

	x=0	x=0.1	x=0.2	x=0.3	x=0.4	x=0.5	x=0.6	x=0.7
y=0 Amma	5.8	6.7	5.7	5.3	5.6	5.9	6.1	6.2
y=0 F222	6.7	6.2	5.3	4.9	5.0	5.1	5.3	5.5

Difference in the obtained R_{wp} values are not very large but systematically small for the F222 model in the case of x=0.1 – 0.7 samples. It was reasonable to assume that the suitable model for the x=0.0 and other samples are different, i.e., Amma and F222, respectively in the present system, being consistent with the literature[5-9]. Figure 5 shows the fitted ND pattern of x=0 and y=0 sample. Solid line and dots represent the calculated intensities and the observation, respecttively. Agreement between the calculation and the observations seems to be good. Figure 6 shows a schematic presentation of the crystal structure of present misfit layered oxide $[(Sr_{1-x}Ca_x)_2Cu_2O_3]_\gamma[Cu_{1-y}Co_yO_2]$. Nearly flat Cu_2O_3 ladder planes and twisted CuO_2 chains are seen. Vertical lines connecting between the ladders and chains represent the chemical bonds, being shorter than 2.8 Å, between the copper and apical oxygen, O3, ions of CuO_5 pyramids. The Cu-O3 distance decreases with increasing calcium and cobalt contents. Figure 7 represents the Cu-O1, CuO2 and Cu-O3 interatomic distances as a function of the phase factor , t'= $-(c_2/c_1)X_3+X_4$, where X_3 and X_4 represent the coordinates parallel to the c_1- and c_2-axes of the two subsystems. The Cu-O3 distance is more than 3.1 Å in the calcium free end member, the left panel of the Fig.7, becomes less than 2.8 Å, just partly though, in the right panel, x=0.7 and y=0.0. The Cu-O1 and Cu-O2 distances are the ones in the ladder plane, decreasing gradually by the decrease of a- and b-axes in the doped system. In the samples with y>0.0, it is indicated that the cobalt ions only substitute the chain-site copper ions rather than the ladder-sites.

III-3. THERMOELECTRIC PROPERTIES

The electrical resistivity, Seebeck coefficient and the power factor were measured for the present layered oxides from 80K to 300K. Figures 8 and 9 show the electrical resistivity of x=0.0 – 0.8 with y=0.2 samples and Seebeck coefficient of x=0.5 and y=0.0 – 0.2 samples, respectively. The electrical resistivity vs. temperature curves show that the present samples are semiconducting in above temperature range.

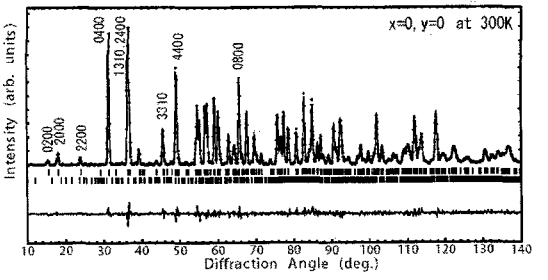

Fig.5 Powder ND pattern of x=0 and y=0 sample.

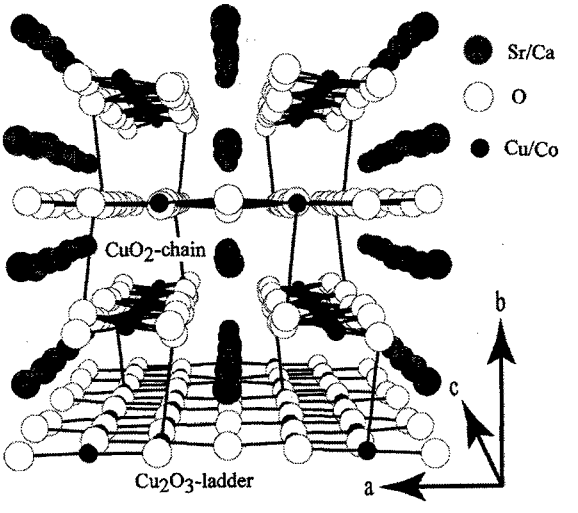

Fig.6 Schematic presentation of obtained crystal structure of the misfit layered oxide, $[(Sr_{1-x}Ca_x)_2Cu_2O_3]_\gamma[Cu_{1-y}Co_yO_2]$.

For example, the observed electrical resistivity of the x=0.8 and y=0.2 sample is about 0.9 Ωcm at 80K but becomes 20m Ωcm at 300K, rather high for the thermoelectric devices. Seebeck coefficient is positive from 80K to 300K, decreasing

from a relatively high value at low temperature to a low one at 300K, e.g., 500 μ V/K for the x=0.5 and y=0.2 sample

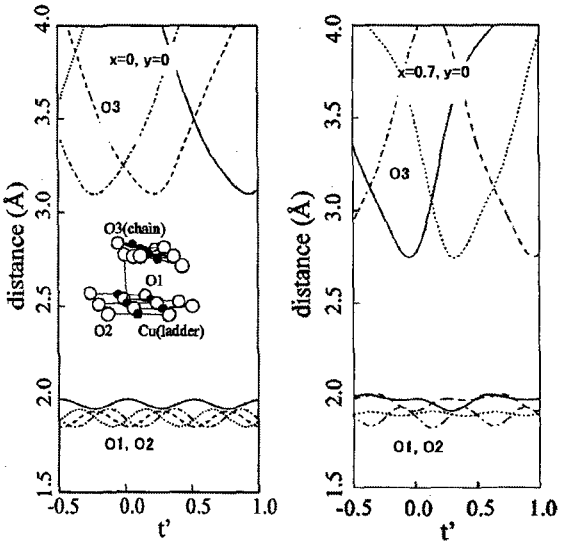

Fig.7 Obtained interatomic distances between copper and the nearest oxygen atoms, O1, O2 and O3, as a function of the phase factor, $t' = -(c_2/c_1)X_3+X_4$, where X_3 and X_4 represent the coordinates parallel to the c_1- and c_2-axes of the two subsystems.

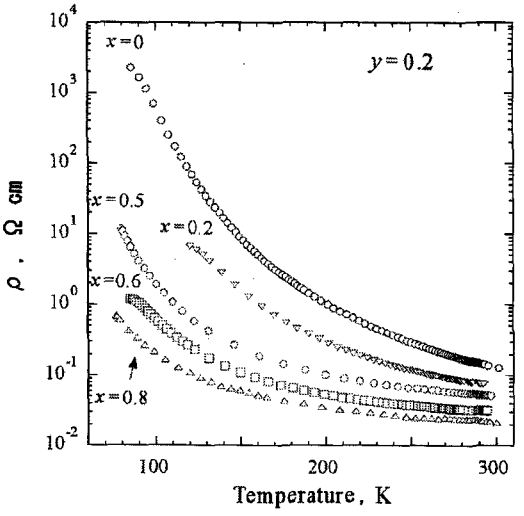

Fig.8 Electrical resistivity of x=0.0 – 0.8, y=0.2 samples.

at about 80K decreases to 180 μ V/K at 300K. The electrical resistivity vs. temperature dependencies are analyzed in terms of the variable range hopping scheme[17]. Decreasing electrical resistivity of the doped samples is interpreted in terms of the decreasing copper-oxygen distances in the ladder - and chain-subsystems. Inhomogeneous spin arrangement in the cobalt doped samples is a possible answer for the increasing electrical resistivity. Since the electric current is due to the simultaneous flow of charges and spins, scattering probability

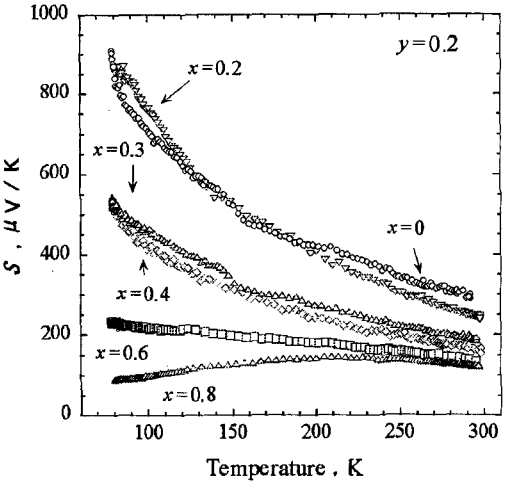

Fig9.Seebeck coefficient of x=0-0.8, y=0.2 samples.

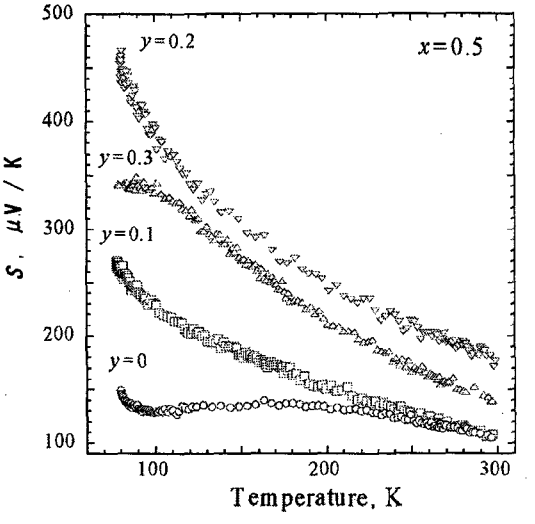

Fig.10 Seebeck coefficient of x=0.5, y=0.0 – 0.3 samples.

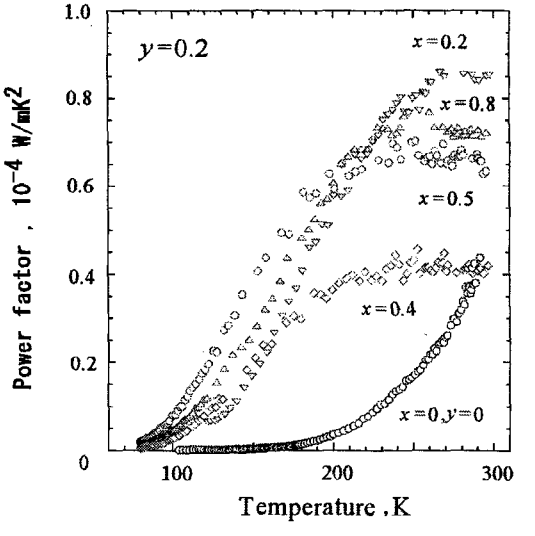

Fig.11 The power factor of x=0.0 – 0.8, y=0.2 samples below 300K.

carriers increases by the inhomogeneous spin arrangement. The Seebeck coefficient was expected to be enhanced by the substitution of high-spin cobalt ions for copper sites. Seebeck coefficient decreases with increasing x (calcium content) and y (cobalt content) in the range $x \leqq 0.4$. In the high calcium range with $x \geqq 0.5$, Seebeck coefficient increases with increasing y up to the range of $y \leqq 0.3$. The maximum value of the power factor, S^2/ρ (W/mK^2) = 0.85×10^{-4}, of the present samples was recorded at x=0.2 and y=0.2 in the temperature range $260K \leqq T \leqq 300K$. The second highest power factor, 0.75W/mK^2, is observed in a sample, x=0.2 and y=0.8 at about 250K

Between 300K to 1000K, the electrical resistivity and Seebeck coefficient were measured for some typical samples. Figure 12 shows obtained power factors in the range

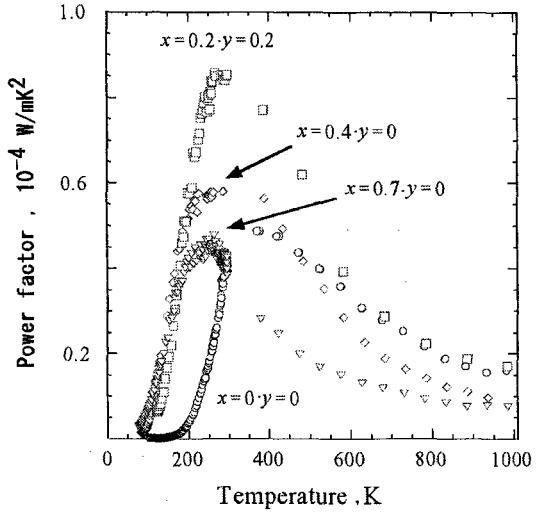

Fig.12 The power factor of typical samples at temperatures from 80K to 1000K.

from 80K to 1000K. The highest values are obtained at about 300K for the measured samples. Above 300K, the power factor decreases with increasing temperature. The thermal conductivity, κ (W/mK), of the calcium doped single crystalline $[(Sr_{1-x}Ca_x)_2Cu_2O_3]_\gamma[Cu_{1-y}Co_yO_2]$ with y=0 were measured by Sologubenko et al.[18] and Kudo et al.[19]. Very anisotropic values in the parallel and perpendicular to the conducting directions were noticed by two groups, namely, about 13 and 2 W/mK[18] at 300K for x=0.125 sample , respectively. The lowest and the highest values, 0.9W/mK and 9.5W/mK at the same temperature range, were observed for the sample with x=0.19 by Kudo et al.[19], being lower in the higher calcium samples. If we can average these anisotropic thermal conductivity for the polycrystalline samples, we will be able to assume the *ZT* value of x=0.2 (y=0.2) sample, as *ZT*=6x10^{-3} at about 300K.

IV. CONCLUSIONS

Title misfit layered cuprate shows relatively high thermoelectric properties from 80K to 300K by the calcium and cobalt co-doping. Dramatic decrease of electrical resistivity was observed by the calcium doping as in the superconducting cuprate[1,2]. The maximum power factor , S^2/ρ (W/mK^2) = 0.85×10^{-4}, is observed in the case of x=0.2, y=0.2 at temperatures in the range $260K \leqq T \leqq 300K$ However, the power factor of the oxide $[(Sr_{1-x}Ca_x)_2Cu_2O_3]_\gamma[Cu_{1-y}Co_yO_2]$ seems to decrease from 300K to 1000K with increasing temperature. The maximum ZT value at about 300K, 6x10^{-3} , of this system is estimated from the literature value of the thermal conductivity.

ACHNOWLEDGEMENT

Present work was partly supported by CREST project of Japan Science and Technology Corporation (JST) and Grand-in-Aid (14505095) for Scientific Research of the Ministry of Education, Science, Sports and Culture of Japan.

REFERENCES

[1] M.Uehara, T.Nagata, J.Akimitsu, H.Takahashi, N.Mori and K.Kinoshita; J.Phys.Soc.Jpn 65, 2764-2767 (1996).
[2] M.Kato, K.Shiota, Y.Koike; Physica C 258, 284-292 (1996).
[3] K.Kato, E.Takayama-Muromachi, K.Kosuda and Y.Uchida; Acta Cryst. C44, 1881-1884 (1988).
[4] K.Kato; Acta Cryst. B46, 39-44 (1990).
[5] T.Ohta, F.Izumi, M.Onoda, M.Isobe, E.Takayama-Muromachi and A.W.Hewat; J.Phys.Soc. Jpn 66, 3107-3114(1997).
[6] Y.Gotoh, Y.Takahashi, J.Akimoto, S.Mizuta, M.Onoda, H.Fujino, T.Nagata and J.Akimitsu; Physica C 341-348, 469-470 (2000).
[7] M.Isobe, M.Onoda, T.Ohta, F.Izumi, K.Kimoto and E.Takayama-Muromachi; Phys.Rev.B62,11667-11676 (2000).
[8] A.F.Jensen, F.K.Larsen, N.B.Iversen, V.Petric, T.Schultz and Y.Gao; Acta Cryst.B53,113-124 (1997).
[9] A.F.Jensen, V.Petric,F.K.Larsen and E.M.McCarron(III);Acta Cryst.B53,125-134 (1997).
[10] S.Li, R.Funahashi, I.Matsubara, K.Ueno and H.Yamada; J.Mater.Chem. 9,1659-1666 (1999).
[11] Y.Miyazaki, K.Kudo, M.Akoshima, Y.Ono, Y.Koike and T.Kajitani; J.Appl.Phys. 39, L531-L533 (2000).
[12] W.Koshibae, K.Tsutsui and S.Maekawa; Phys.Rev.B 62, 6869-6872 (2000).
[13] W.Koshibae and S.Maekawa; Phys.Rev. Letters 87,236603-1-236603-4, (2001).

[14] K.Ohyama, T.Kanouchi, K.Nemoto, M.Ohashi, T.Kajitani and Y.Yamaguchi; Jpn.J.Appl.Phys. 37,3319-3326(1998).
[15] A.Yamamoto; Acta Cryst. A 49, 831-846 (1993).
[16] R.D.Shannon and C.T.Prewitt; Acta Cryst. B25,925-946 (1969).
[17] M.Uehara, M.Ogawa, J.Akimitu; Physica C 255,193-203 (1995).
[18]A.V.Sologubenko, K.Gianno, H.R.Ott, U.Ammerahl, A.Revolevschi, B.F.Brewer and A.L.Thomson; Physica B 284-288, 1595-1596 (2000).
[19] K.Kudo, S.Ishikawa, T.Noji, T.Adachi, Y.Koike, K.Maki, S.Tsuji and K.Kumagai; J.Phys.Soc. Jpn 70,437-444 (2001).

APPNEDIX

Refined structural parameters of $[(Sr_{1-x}Ca_x)_2Cu_2O_3]_g[Cu_{1-y}Co_yO_2]$ with x=0.7 and y=0 at 300K A0 terms are the constants characteristic for the 3-dimensional fundamental lattices. A1 and A2 represent the amplitudes of the primary and the secondary "cosine" displacement waves. B1 and B2 represent the amplitudes of the primary and the secondary "sine" displacement waves, respectively.

Spacegroup : F222(00γ)001 : a=11.3206(5) Å , b=12.7056(6) Å, c1=3.9011(2) Å, c2=2.7496(2) Å , γ =0.7048(1)

$(Sr_{0.30}Ca_{0.70})_2Cu_2O_3$ subsystem

Atom	A0	A1	B1	A2	B2
Sr(Ca)					
x	1/2	0	-0.003(1)	0	-0.01(6)
y	0.380(1)	-0.010(3)	0	0.002(3)	0
z	3/4	0	-0.01(12)	0	0.004(12)
B	0.75(17)	0	0	0	0
Cu1					
x	0.3342(4)	–0.000(4)	0	0.005(2)	0
y	1/4	0	-0.005(1)	0	-0.001(9)
z	1/4	0	-0.003(9)	0	-0.001(9)
B	0.46(13)	0	0	0	0
O1					
x	0.1668(6)	–0.001(5)	0	0.004(3)	0
y	1/4	0	-0.008(1)	0	0.009(3)
z	1/4	0	0.006(12)	0	0.007(13)
B	0.5(22)	0	0	0	0
O2					
x	1/2	0	0	0	0
y	1/4	0	0	0	0
z	1/4	0	-0.015(15)	0	-0.007(18)
B	1.37(31)	0	0	0	0

CuO_2 subsystem

Atom	A0	A1	B1	A2	B2
Cu2					
x	1/4	0	0	0	0
y	1/2	0	0	0	0
z	1/4	0	0.024(13)	0	-0.022(8)
B	1.68(20)	0	0	0	0
O3					
x	0.1353(4)	0.003(3)	0	0.002(1)	0
y	1/2	0	0.0264(9)	0	-0.005(3)
z	3/4	0	0.038(13)	0	0.001(7)
B	1.72(20)	0	0	0	0

(Received October 13, 2003; Accepted January 16, 2004)